

Periostin, a Cell Adhesion Molecule, Facilitates Invasion in the Tumor Microenvironment and Annotates a Novel Tumor-Invasive Signature in Esophageal Cancer

Carmen Z. Michaylira^{1,2,5}, Gabrielle S. Wong^{1,2,5}, Charles G. Miller^{1,2,5}, Christie M. Gutierrez^{1,2,5}, Hiroshi Nakagawa^{1,2,5}, Rachel Hammond^{5,6}, Andres J. Klein-Szanto⁷, Ju-Seog Lee⁹, Sang Bae Kim⁹, Meenhard Herlyn⁴, J. Alan Diehl^{5,8}, Phyllis Gimotty^{5,6}, and Anil K. Rustgi^{1,2,3,5}

Abstract

Human squamous cell cancers are the most common epithelially derived malignancies. One example is esophageal squamous cell carcinoma (ESCC), which is associated with a high mortality rate that is related to a propensity for invasion and metastasis. Here, we report that periostin, a highly expressed cell adhesion molecule, is a key component of a novel tumor-invasive signature obtained from an organotypic culture model of engineered ESCC. This tumor-invasive signature classifies with human ESCC microarrays, underscoring its utility in human cancer. Genetic modulation of periostin promotes tumor cell migration and invasion as revealed in gain-of-loss and loss-of-function experiments. Inhibition of epidermal growth factor receptor signaling and restoration of wild-type p53 function were each found to attenuate periostin, suggesting the interdependence of two common genetic alterations with periostin function. Collectively, our studies reveal periostin as an important mediator of ESCC tumor invasion and they indicate that organotypic (three-dimensional) culture can offer an important tool to discover novel biological effectors in cancer. *Cancer Res*; 70(13); 5281–92. ©2010 AACR.

Introduction

The development of esophageal squamous cell carcinoma (ESCC) involves a multistep, progressive process starting with increased esophageal epithelial cell proliferation leading to basal cell hyperplasia, dysplasia, carcinoma *in situ*, and, finally, advanced invasive carcinoma (1–3). Several genetic alterations, such as amplification of the epidermal growth factor (EGF) receptor (EGFR), dysregulation of cyclin D1, and somatic mutations in the DNA binding domain of the tumor suppressor p53, are involved in initiation and progression of ESCC (4). Although EGFR overexpression and p53 inactivation are key genetic alterations associated with ESCC, how these genetic alterations contribute to ESCC progression remains to be elucidated. Previously, we had addressed this by

modeling EGFR overexpression and p53 missense mutation (R175H) in primary human esophageal epithelial cells (EPC2), which have been immortalized by hTERT overexpression (designated as EPC2-hTERT-EGFR-p53^{R175H} cells). EPC2-hTERT-EGFR-p53^{R175H} cells were grown in three-dimensional organotypic culture, resulting in the invasion of these cells into the underlying extracellular matrix (ECM) compared with EPC2-hTERT-EGFR or EPC2-hTERT-p53^{R175H} cells, which did not invade (5). Combined expression of these genes also resulted in anchorage-independent growth and in tumor formation in xenograft models, which was not observed in control cells overexpressing either EGFR or mutant p53 alone (5).

Recent experimental results have provided mounting evidence that altered expression of cell adhesion molecules can contribute directly to tumor progression by modulating cell signaling. Therefore, we sought to identify genes involved in cell adhesion that were differentially expressed in invading tumor cells and could shed new insights into processes affecting tumor progression.

Deriving a novel invasive tumor signature from a gene expression profile analysis of invading EPC2-hTERT-EGFR-p53^{R175H} cells in three-dimensional culture and human ESCC tumor microarrays, we have identified periostin to be the most significantly upregulated gene triggering tumor cell invasion. Periostin (*POSTN*) is a secreted 90-kDa protein that was identified originally as a bone adhesion molecule responsible for differentially recruiting and attaching osteoblasts to the periosteum (6). Periostin is a member of the fasciclin

Authors' Affiliations: ¹Division of Gastroenterology, Departments of ²Medicine, ³Genetics, and ⁴Cancer Biology, ⁵Abramson Cancer Center, and ⁶Division of Biostatistics, Center for Clinical Epidemiology and Biostatistics, University of Pennsylvania; ⁷Division of Basic Science, Tumor Cell Biology, Fox Chase Cancer Center; and ⁸Wistar Institute, Philadelphia, Pennsylvania; and ⁹Department of Systems Biology, M.D. Anderson Cancer Center, Houston, Texas

Note: Supplementary data for this article are available at Cancer Research Online (<http://cancerres.aacrjournals.org/>).

C.Z. Michaylira and G.S. Wong contributed equally to this work.

Corresponding Author: Anil K. Rustgi, 600 CRB University of Pennsylvania, 415 Curie Boulevard, Philadelphia, PA 19104. Phone: 215-898-0154; Fax: 215-573-5412; E-mail: anil2@mail.med.upenn.edu.

doi: 10.1158/0008-5472.CAN-10-0704

©2010 American Association for Cancer Research.

family and has a NH₂-terminal signal peptide sequence, a cysteine-rich domain, four internal homologous repeats, and a hydrophilic COOH-terminal domain (6). These four internal repeat domains share structural homology with Fasciclin 1, an insect neuronal adhesion protein (6, 7), and big-h3, a transforming growth factor- β 1 (TGF β 1)-inducible gene (7, 8). The high degree of structural and sequence similarity with these cell adhesion molecules suggests that periostin has a role in cell adhesion and migration. Indeed, not only is its expression induced in human ESCC and mouse tumor xenografts, but more importantly, genetic modulation of periostin also affects tumor invasion in a direct fashion. The novel identification of periostin as an essential mediator of tumor invasion in the microenvironment has implications upon tumor detection and therapy.

Materials and Methods

Cell culture

Primary esophageal cells (EPC2) were established from surgical specimens of normal esophagus as previously described (9) and immortalized by overexpression of the catalytic subunit of telomerase (hTERT; EPC2-hTERT cells; ref. 10). All cells were maintained in keratinocyte-SFM medium (Invitrogen) supplemented with 40 mg/mL BPE, 1.0 ng/mL EGF, 100 U/mL penicillin, and 100 mg/mL streptomycin (full keratinocyte-SFM medium). Cells were grown at 37°C in 5% CO₂.

Retroviral vectors and cell line generation

The PFB-neo or pBABE-zeo retroviral vectors were used to overexpress human EGFR in EPC2-hTERT cells. Additionally, p53^{R175H} was subcloned into the pBABE-puro or the pBABE-zeo retroviral vectors. Periostin cDNA was used (Open Biosystems) and subcloned into the pFBneo retroviral vector. Two periostin short hairpin RNAs (shRNA#1 5'-CCCATGGAGAGCCAATTAT-3' and shRNA#2 5'-CTCTGACATCATGACAACAAAT-3') were used (Open Biosystems). Plasmids were transfected into Phoenix-Ampho packaging cells (gift of G. Nolan, Stanford University, Palo Alto, CA) using the Lipofectamine 2000 reagent (Invitrogen). Supernatants of the retroviruses encoding EGFR, mutant p53, periostin overexpression, and shRNA vector constructs were collected 48 and 72 hours after transfection. Subconfluent EPC2-hTERT cells were infected with retrovirus supernatant in 4mg/mL polybrene (Sigma). Forty-eight hours after infection, cells were selected in 300 μ g/mL G418, 0.5 μ g/mL puromycin, 2 mg/mL zeocin, or 5 mg/mL blastocidin for 5 days. Overexpression of EGFR, mutant p53, and periostin, as well as periostin knockdown was confirmed by Western blot analysis.

Organotypic culture

Keratinocytes were grown in organotypic culture to recreate their microenvironment by supplying ECM components including collagen, and laminin and fetal esophageal fibroblasts; its detailed procedures were previously described (5). Cells grown in organotypic culture were processed for histology by fixing in 10% formaldehyde and were paraffin

embedded for laser capture microdissection (LCM) studies by embedding in OCT medium followed by freezing in liquid nitrogen and then stored at -80°C.

LCM and RNA isolation

Frozen organotypic cultures were sectioned to 8 μ m onto membrane-mounted metal frame slides (MMI) using a Microm HM 505E cryostat (Richard Allen Scientific). Sections were immediately fixed, stained, and dehydrated before laser microdissection. Microdissection was performed with a Nikon Eclipse TE 2000-5 microscope with a UV laser (MMI). Microdissected cells were collected, and 50 μ L of extraction buffer (Arcturus) were added and incubated for 30 minutes at 42°C, followed by centrifugation at 800 \times g for 2 minutes. RNA was extracted using the Arcturus PicoPure RNA isolation kit following the manufacturer's instructions. The integrity and concentration of the RNA was assessed using the Agilent Bioanalyzer 2100 (Agilent Technologies).

RNA amplification and microarray studies

The RNA obtained from the LCM studies was amplified using the Affymetrix GeneChip Expression 3'-Amplification Two-Cycle cDNA Synthesis kit (Affymetrix) followed by the Affymetrix GeneChip Hybridization Wash and Stain kit (Affymetrix). The resulting cRNA (200 ng) was used as template for random-primed cDNA synthesis and a second round of *in vitro* transcription, which incorporated biotinylated CTP and UTP. The cRNA products were fragmented to 200 bp or less, heated at 99°C for 5 minutes, and hybridized for 16 hours at 45°C to Affymetrix U133Plus 2.0 oligonucleotide microarrays (Affymetrix). Microarrays were subsequently washed at low (6 \times saline-sodium phosphate-EDTA) and high (100 mmol/L MES, 0.1 mol/L NaCl) stringency, and stained with streptavidin-phycoerythrin. The fluorescence signal was amplified by the addition of biotinylated anti-streptavidin and an additional aliquot of streptavidin-phycoerythrin stain. A confocal scanner was used to acquire the fluorescent signal after excitation (570 nm).

Quantitative PCR

LCM was repeated to isolate invading and noninvading EPC2-hTERT-EGFR-p53^{R175H} cells grown in organotypic culture. Amplification and cDNA synthesis was performed using WT-Ovation RNA Amplification System (NuGen Technologies) according to the manufacturer's instructions. Real-time PCR was performed and analyzed using the ABI PRISM 7000 sequence detection system software (PE Applied Biosystems) and using the Power SYBR Green PCR Master Mix (PE Applied Biosystems) for β -actin according to the manufacturer's instructions. Taqman assays for periostin were run using the Taqman Universal PCR Master Mix (PE Applied Biosystems) according to the manufacturer's instructions.

Tumor specimens

Esophageal tumor tissue specimens and adjacent normal tissue were surgically procured from patients at the Okayama University Hospital (Drs. Shirakawa and Naomoto, Japan). All tumor specimens were pathologically diagnosed as ESCCs

(grade III) and obtained from patients who signed informed consents in accordance with Institutional Review Board standards and guidelines.

Specimens were immediately snap frozen for RNA and protein analyses. The human ESCC tissue microarray was subjected to immunohistochemistry analysis using a polyclonal anti-periostin antibody and scored for periostin expression as follows; negative (0), marginal considered negative (0.5), mild positive stain (1), moderate positive stain (2), and intense positive stain (3). Scores of >0.5 are considered positive. Each case on the tissue microarray comprises of two cores and the mean scores of two cores were taken.

Antibodies

The following antibodies were used for immunoblotting: EGFR (NeoMarkers, Ab-12), p53 (Oncogene Research Products, Ab-6), phospho-EGFR (Cell Signaling, Tyr 1068), rabbit polyclonal periostin (Abcam, ab 14041), and p21 (Oncogene Research Products), WAF1 (ab-1); β -Actin (Sigma) was used as a loading control. For immunohistochemistry, periostin (Abcam, ab 14041) was used.

Western blotting

To confirm protein expression, Western blot analysis was performed as previously described (5). To confirm secreted periostin expression, conditioned media was collected, protein concentration was determined by Bio-Rad protein assay (Bio-Rad), and Western blot analysis was performed as described above.

Migration and invasion assays

Migration and invasion assays were performed as previously described (5). All experiments were performed at least three times in triplicate.

Data processing

Affymetrix array cel files were processed in R using an algorithm that uses genes in the least variant set to normalize the expression data (11). In the analysis of invasive and non-invasive cells, we then identified 6,106 probe sets for subsequent statistical analysis that had a minimum expression level (expression of >100 in all samples) and that had significant variability among the 11 cell lines (SD was >150). The background correction, summarization, and normalization of Affymetrix cel files were done in the same manner independently for each of the two tumor/normal studies. Gene Expression Omnibus database accession number is GSE21293.

Statistical analysis

All statistical analyses used natural log-transformed expression data. Using the arrays of cells from the organotypic culture model, a multivariate regression model was fit for each gene that included two independent binary variables. The first variable indicated cells with both EGFR overexpression and P53 mutation only and the second indicated cells with EGFR overexpression, P53 mutation, and invasion. The third group (the reference group) included cells with a non-invasive phenotype that had either EGFR overexpression or

P53 mutation. The *P* values from the test that the regression model was significant (F-statistic, 2 degrees of freedom) were adjusted using the Benjamini-Hochberg technique; probe sets with a false discovery rate of <0.05 were selected for further investigation (12). Genes on this list were compared with annotated gene ontology (GO) biological processes, and a functional annotation cluster analysis was done using the online DAVID tool (<http://niaid.abcc.ncifcrf.gov/>). Annotations were derived from the DAVID databases. Supervised hierarchical clustering used in the heat maps was based on the Euclidean distance. The statistical analyses were done using the SAS/STAT software version 9.2 of the SAS System for personal computer.

Results

Identification of periostin from tumor invasion signature derived from gene expression profile analysis on invading EPC2-hTERT-EGFR-p53^{R175H} cells and ESCC tumor microarrays

The molecular pathways and networks underlying tumor invasion remain largely to be elucidated. To characterize a gene expression profile underlying the invasive phenotype of invading EPC2-hTERT-EGFR-p53^{R175H} cells, we profiled mRNA obtained from laser capture-microdissected EPC-hTERT cells overexpressing EGFR and with a p53 missense mutation (R175H) that was either invasive or noninvasive in the organotypic culture model, as well as noninvasive cells that either overexpressed EGFR alone or had p53 (R175H) mutation alone, using Affymetrix U133-2 plus microarrays.

Analysis of the gene expression microarray data revealed a tumor-invasive signature corresponding to a probe set list of 939 probe sets, in which there was significant differential expression of these probe sets in invasive versus noninvasive cells (Supplementary Table S1). A supervised hierarchical cluster analysis showed that this tumor-invasive signature could distinguish significant differences between cell lines in organotypic culture with and without an invasive phenotype as presented in a heat map (Fig. 1A).

To determine whether this invasive signature derived from invading EPC2-hTERT-EGFR-p53^{R175H} cells grown in organotypic culture can be extended to human ESCC, we analyzed gene expression profiles from five paired human ESCCs. We found that overall gene expression patterns of invasive cells grown in organotypic culture are highly similar to those from ESCC tumors, and this tumor-invasive signature was able to discriminate esophageal tumors from adjacent normal tissue and classified all tumors and 80% of the normal samples correctly (Fig. 1B). To validate this tumor-invasive signature, we performed a secondary analysis on an independent cohort of five paired human ESCC tumors using this tumor-invasive signature and observed that it was capable of classifying 80% of ESCC tumors and all adjacent normal tissues correctly (Fig. 1C). Using the *t* test statistic to rank the probe sets in this tumor-invasive signature, we identified periostin, a cell adhesion molecule, with the most significant difference in gene expression between invading transformed esophageal epithelial cells compared with noninvading

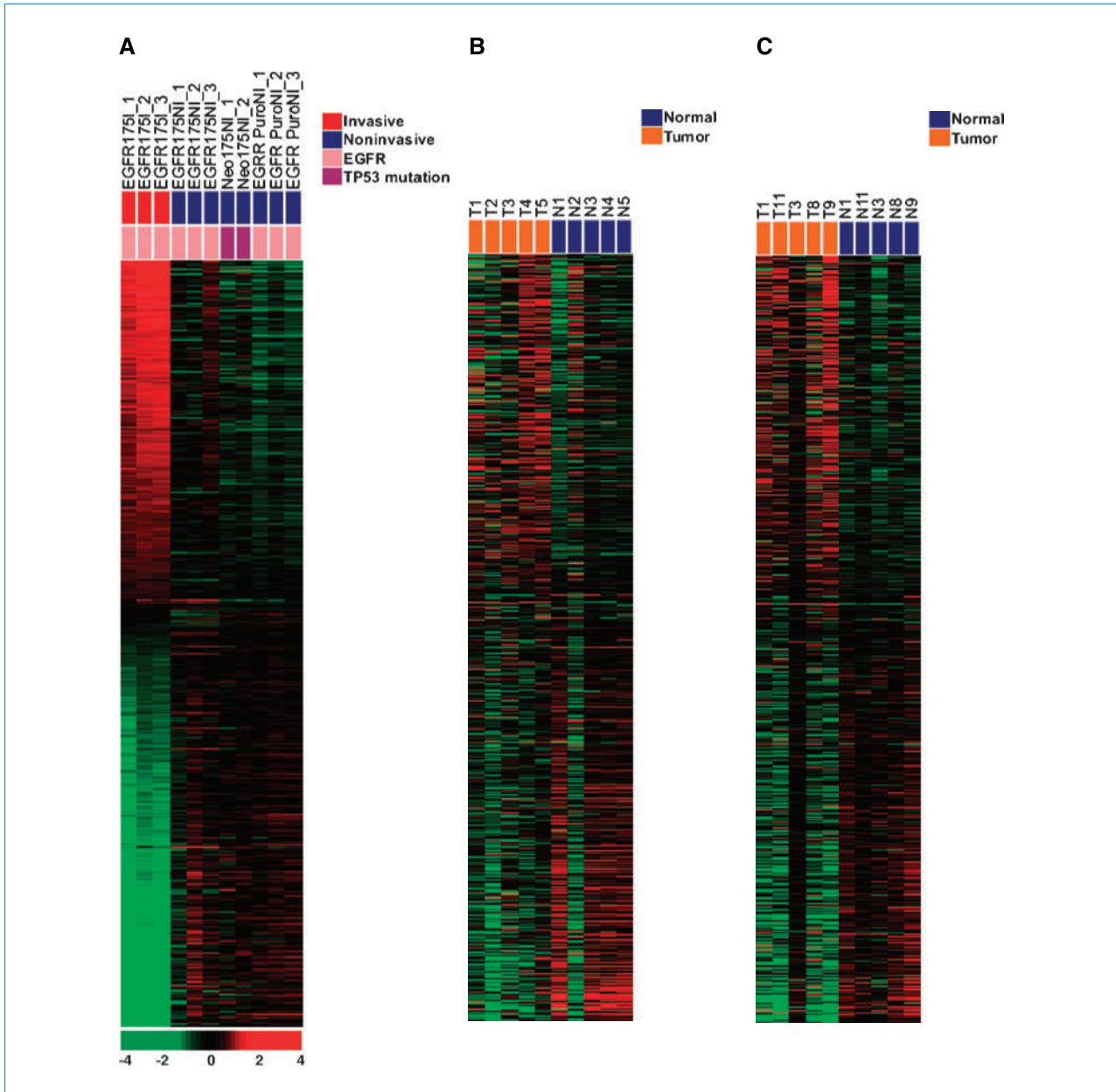


Figure 1. Invasive signature from EPC2-hTERT-EGFR-p53^{R175H} cells classifies with human ESCC. A, microarray analysis of LCM-extracted RNA from invading EPC2-hTERT-EGFR-p53^{R175H} cells grown in organotypic culture ($n = 3$) compared with noninvading EPC2-hTERT-EGFR-p53^{R175H} ($n = 3$) as well as noninvading EPC2-hTERT-EGFR-puro ($n = 3$) and EPC2-hTERT-neop53^{R175H} cells ($n = 2$). Differentially expressed probe sets were subjected to supervised hierarchical clustering, and expression is based on a log₂ scale in which red represents upregulation and green represents downregulation. Heat map denotes a probe set list of 939 probe sets representing unique tumor-invasive signature characterizing invasive phenotype. Tumor invasive signature comprises differentially expressed probe sets ($P < 0.0001$). B and C, heat map representation of gene-expressing profiles from two independent cohorts each comprising of five paired ESCC tumors classified using the tumor-invasive signature from A. Due to microarray platform difference (U133 v2.0 and U133A) used in two independent cohorts, only 648 probe sets were shared in both platforms. All probe sets are in the same order as seen in A.

normal or dysplastic epithelial cells (t test for two independent groups, $P < 0.0001$). Strikingly, periostin was also found to be significantly upregulated in both independent cohorts of human ESCC tumors compared with adjacent normal tissue; the fold change in mean periostin expression was found to be 5.0 and 5.7 in the respective cohorts.

To explore the biological processes associated with invasion of ESCC, we tested for enrichment of GO terms within this tumor-invasive signature. This tumor-invasive signature was found to be significantly enriched in nine biological processes (false discovery rate, $P < 0.01$; data not shown; Supplementary Table S1 and S2). To investigate the cellular

Table 1. Gents with at least 2-fold higher expression in invasive EPC2.hTERT.EGFR.p53R175H cell lines compared with noninvasive EPC2.hTERT.EGFR.p53R175HEPC2.hTERT.EGFR.puro.EPC:2.hTERT.neo.p53R175H cell lines by GO Biological Processes

Cellular component organization and biogenesis GO:0016043			Biological adhesion and cellular adhesion GO:0022610 and GO:0007155			Developmental processes GO:0048856,0032502,0048731,0009888;0048513 and 0007275		
Probe set	Gene name	Ratio*	Probe set	Gene name	Ratio*	Probe set	Gene name	Ratio*
210809_s_at	POSTN	6.54	210809_s_at	POSTN	6.54	210809_s_at	POSTN	6.54
211964_at	COL4A2	4.28	226237_at	COL8A1	5.43	206300_s_at	PTHLH	4.01
216250_s_at	LPXN	4.17	201109_s_at	THBS1	5.11	212667_at	SPARC	3.72
210511_s_at	INHBA	3.93	204955_at	SRPX	4.61	209270_at	LAMB3	3.27
201162_at	IGFBP7	3.72	216250_s_at	LPXN	4.17	202267_at	LAMC2	2.76
231766_s_at	COL12A1	3.67	209651_at	TGFB111	4.15	229404_at	TWIST2	2.65
213869_x_at	THY1	3.60	227566_at	HNT	3.98	200827_at	PLOD	2.24
201389_at	ITGA5	3.50	231766_s_at	COL12A1	3.67	213139_at	SNAI2	2.14
202760_s_at	AKAP2	3.47	213869_x_at	THY1	3.60	203695_s_at	DFNA5	2.07
201645_at	TNC	3.44	201389_at	ITGA5	3.50			
203562_at	FEZ1	3.37	201645_at	TNC	3.44			
224911_s_at	DCBLD2	3.31	203562_at	FEZ1	3.37			
212233_at	MAP1B	3.26	224911_s_at	DCBLD2	3.31			
209210_s_at	PLEKHC1	3.24	209270_at	LAMB3	3.27			
230175_s_at	ESDN	3.08	209210_s_at	PLEKHC1	3.24			
205120_s_at	SGCB	2.94	212489_at	COL5A1	3.17			
221916_at	NEFL	2.93	202998_s_at	LOXL2	3.15			
204682_at	LTBP2	2.89	230175_s_at	ESDN	3.08			
37408_at	MRC2	2.87	52255_s_at	COL5A3	3.02			
219257_s_at	SPHK1	2.86	212464_s_at	FN1	2.93			
218638_s_at	SPON2	2.74	211340_s_at	MCAM	2.79			
208637_x_at	ACTN1	2.72	202267_at	LAMC2	2.76			
224252_s_at	FXYD5	2.66	218638_s_at	SPON2	2.74			
204466_s_at	SNCA	2.61	208637_x_at	ACTN1	2.72			
218980_at	FHOD3	2.56	222108_at	AMIGO2	2.71			
218368_s_at	TNFRSF12A	2.55	205534_at	PCDH7	2.66			
208079_s_at	STK6	2.53	224252_s_at	FXYD5	2.66			
201042_at	TGM2	2.53	218368_s_at	TNFRSF12A	2.55			
202095_s_at	BIRC5	2.51	201042_at	TGM2	2.53			
201505_at	LAMB1	2.48	204359_at	FLRT2	2.52			
202796_at	SYNPO	2.47	201505_at	LAMB1	2.48			
210026_s_at	CARD10	2.47	204345_at	COL16A1	2.47			
221748_s_at	TNS	2.40	242064_at	SDK2	2.45			
203131_st	PDGFRA	2.35	201474_s_at	ITGA3	2.35			
218644_at	PLEK2	2.32	226609_at	DCBLD1	2.29			
221898_st	T1A-2	2.27	225293_at	COL27A1	2.15			
201185_at	PRSS5	2.23						
204170_s_at	CKS2	2.22						
211725_s_at	BID	2.20						
201540_at	FHL1	2.13						
214752_x_at	FLNA	2.03						

*Multivariate logistic regression models were used to test each probe set and adjusted for false discovery rate ($P < 0.01$).

processes altered within the tumor microenvironment, we selected three biological processes for further investigation and observed that probe sets clustered in each biological process (cell/biological adhesion, development-related and cellular component organization, and biogenesis) were able to classify invading transformed esophageal epithelial cells from noninvading cells (Supplementary Fig. S1A–C; Table 1). Interestingly, periostin was found to be the highest upregulated gene (6.54-fold) across the three biological processes (Table 1) and was unique in this feature among all the genes in the data sets. In aggregate, these results reveal a tumor-invasive signature derived from the organotypic culture model, which applies faithfully to human ESCC and highlights periostin as an important gene required for facilitating tumor cell invasion.

Periostin is expressed preferentially in invading EPC2-hTERT-EGFR-p53^{R175H} cells both *in vitro* and *in vivo*

We next sought to validate whether the upregulation of periostin is concomitant with invading transformed esophageal cells as well as establishes the localization of periostin expression in these cells. Consistent with the results of the microarray analysis, increased periostin mRNA expression in invading EPC2-hTERT-EGFR-p53^{R175H} cells was confirmed by LCM isolation of invading and noninvading EPC2-hTERT-EGFR-p53^{R175H} cells in the organotypic culture model followed by RNA isolation, amplification, and quantitative PCR analysis (Fig. 2A). Furthermore, periostin pro-

tein accumulation in invading EPC2-hTERT-EGFR-p53^{R175H} cells grown in organotypic culture was observed by immunohistochemical staining (Fig. 2B, right, b) but not in control EPC2-hTERT-EGFR cells (Fig. 2B, left, a). Interestingly, periostin protein expression was also observed in the epithelial-stromal interface in tumors formed by EPC2-hTERT-EGFR-p53^{R175H} cells in a xenograft tumor model (Fig. 2C, white arrows). These results establish the preferential expression of periostin in invading EPC2-hTERT-EGFR-p53^{R175H} cells both *in vitro* and *in vivo*.

Loss of periostin leads to decreased migration and invasion in EPC2-hTERT-EGFR-p53^{R175H} cells

Previous efforts involving other epithelial cancers had indicated that periostin promotes invasion and anchorage-independent growth in several epithelial cancer cell lines and in tumors such as head and neck cell carcinoma, oral, breast, and ovarian cancers (13–16). Elevated levels of periostin have been detected in the sera of patients with breast, thymoma, and non-small cell lung cancer, suggesting periostin secretion during tumorigenesis (17–19). We sought to investigate directly whether periostin had a functional role in facilitating tumor cell migration and invasion in ESCC. An RNA interference approach with shRNA was used to induce stable knockdown of periostin expression in EPC2-hTERT-EGFR-p53^{R175H} cells (Fig. 3A). Knockdown of periostin in EPC2-hTERT-EGFR-p53^{R175H} cells led to significant decrease in cell migration and invasion compared

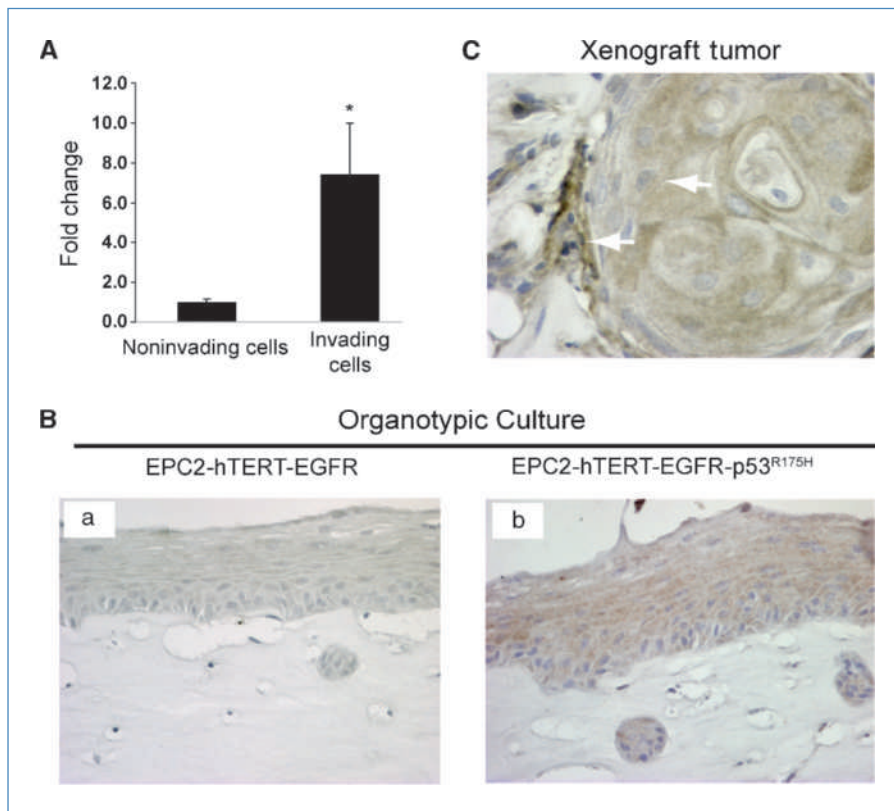


Figure 2. Periostin is expressed preferentially in invading EPC2-hTERT-EGFR-p53^{R175H} cells. A, fold change of periostin expression in invading versus noninvading EPC2-hTERT-EGFR-p53^{R175H} cells isolated by LCM from organotypic culture and quantified by quantitative PCR. *, *P* < 0.05. B, immunohistochemistry analysis of periostin expression in control EPC2-hTERT-EGFR cells (left, a) and invading EPC2-hTERT-EGFR-p53^{R175H} cells (right, b) grown in organotypic culture. Rabbit polyclonal periostin antibody recognizes exogenous and secreted periostin. C, periostin expression by immunohistochemistry of tumor formed *in vivo* by EPC2-hTERT-EGFR-p53^{R175H} cells. White arrows, periostin expression in tumor epithelial-stromal interface. Magnification, ×200.

with control shscrambled cells (Fig. 3B and C). Notably, reduced periostin expression in EPC2-hTERT-EGFR-p53^{R175H} cells also resulted in decreased invasion of these cells into the underlying matrix in organotypic culture (Fig. 3D).

Periostin overexpression promotes increased migration and invasion in EPC2-hTERT-EGFR-p53^{R175H} cells

In parallel studies, periostin was retrovirally overexpressed in two independent cell lines (EPC2-hTERT-EGFR-p53^{R175H}-1 and EPC2-hTERT-EGFR-p53^{R175H}-2; Fig. 4A), and although overexpression of periostin showed no effect on proliferation (data not shown), we observed that these cells displayed increased migration and invasion (Fig. 4B and C). Furthermore, when EPC2-hTERT-EGFR-p53^{R175H} cells overexpressing periostin were grown in organotypic culture, increased invasion into the underlying matrix was also observed (Fig. 4D). Collectively, these results show the direct functional role of periostin in promoting tumor cell migration and invasion, particularly within the context of the tumor microenvironment.

Upregulation of periostin expression in primary ESCC tumors and in a cancer tissue microarray

We next sought to determine if the upregulation of periostin is also found in human ESCC by assessing periostin expression in primary ESCC (grade III) tumors. Increased periostin mRNA expression was observed in ESCC tumors compared with their matched normal controls (Fig. 5A). A marked increase in periostin protein levels was observed in all ESCC tumors studied compared with their matched normal mucosa controls (Supplementary Fig. S2; Fig. 5B). To determine the localization of periostin in human ESCC, further immunohistochemical analysis of periostin expression was performed in a tissue microarray containing 73 ESCC tumors and adjacent normal tissue, and revealed periostin expression in invasive ESCC tumor cells (Fig. 5C, bottom, c, arrowheads) and consistent accumulation in tumor stroma (Fig. 5C, bottom, c, arrows) compared with normal esophageal tissue in which periostin expression was detected primarily in and around blood vessels (Fig. 5C, left, a, arrows). Periostin expression was also detected in high-grade esophageal intraepithelial neoplasia, which was found in a restricted number of cases, particularly in the epithelial-stromal interface (Fig. 5C, right, b, arrows). In addition, the stroma in all 73 ESCC cases were scored for periostin immunohistochemical staining intensity and it was shown to have higher levels of periostin staining compared with matched normal esophagus, which showed weak to no periostin staining. Specifically, the ESCC scored either 2 or 3, meaning moderate or intense staining, whereas the normal esophagus was 0 or 0.5 (Fig. 5C, d), which would suggest that induction of periostin could also arise in the stroma during ESCC progression.

Induction of periostin is dependent on EGFR signaling and p53 mutation

It is believed, but not established, that periostin might enhance tumor cell invasion and metastasis through in-

creased integrin signaling, augmenting cell survival through the phosphoinositide 3-kinase (PI3K)/Akt pathway or fostering epithelial-to-mesenchymal transition (16, 20, 21). Given that periostin was identified initially in invading EPC-hTERT-EGFR-p53^{R175H} cells through functional genomics and bioinformatic analysis, we hypothesized that periostin expression is dependent on both activated EGFR signaling and p53 mutation. Notably, periostin expression was upregulated in EPC2-hTERT-EGFR-p53^{R175H} cells compared with control cells overexpressing EGFR alone (EPC2-hTERT-EGFR) or mutant p53 alone (EPC2-hTERT-p53^{R175H}; Fig. 6A). In addition, periostin promoter reporter assays in EPC2-hTERT-EGFR-p53^{R175H} cells displayed the highest promoter activity compared with control cells with either EGFR overexpression or p53 mutation alone (Supplementary Fig. S3), suggesting that both genetic alterations may be required to activate periostin expression at a transcriptional level. This result was further corroborated when EPC2-hTERT-EGFR-p53^{R175H} cells were stimulated with EGF and increased periostin protein expression was observed (Fig. 6B). This induction of periostin upon EGFR stimulation led us to test whether the inhibition of EGFR signaling and/or restoration of wild-type p53 function could inhibit periostin by treating EPC2-hTERT-EGFR-p53^{R175H} cells. We used AG1478, a EGFR tyrosine kinase inhibitor, and 5-iminodaunorubicin, a small-molecule compound that restores wild-type p53 signaling by inducing apoptosis and cell cycle arrest, as illustrated by the induction of p21(22). Periostin protein expression was noted to be decreased when inhibited by AG1478 or 5-iminodaunorubicin or both (Fig. 6B). Taken together, these data support the notion that periostin expression is modulated mechanistically by activated EGFR signaling and p53 mutation.

Discussion

Overall, our results reveal a novel tumor-invasive signature derived from invading transformed cells compared with control noninvading normal and dysplastic cells in organotypic (three-dimensional) culture. This signature is one that annotates primary invasive human esophageal squamous cell cancer as distinctive from adjacent normal human esophageal mucosa in two independent cohorts of tumors, underscoring the fidelity and utility of this tumor-invasive signature. It is conceivable that this molecular signature might be informative in the future for other squamous cell cancers arising in different tissues.

GO analysis (DAVID databases) of specific biological processes that are believed to be involved in the tumor microenvironment reveals the consistent and unique upregulation of periostin, suggesting its critical functional role. First, periostin was found to be upregulated in invading transformed cells and in primary esophageal squamous cell cancers based on immunohistochemical and Western blot analysis. Second, the direct functional role of periostin is underscored by overexpression and knockdown experiments in which genetic manipulation of periostin dramatically influences the degree of tumor invasion in organotypic culture. Third, EGFR

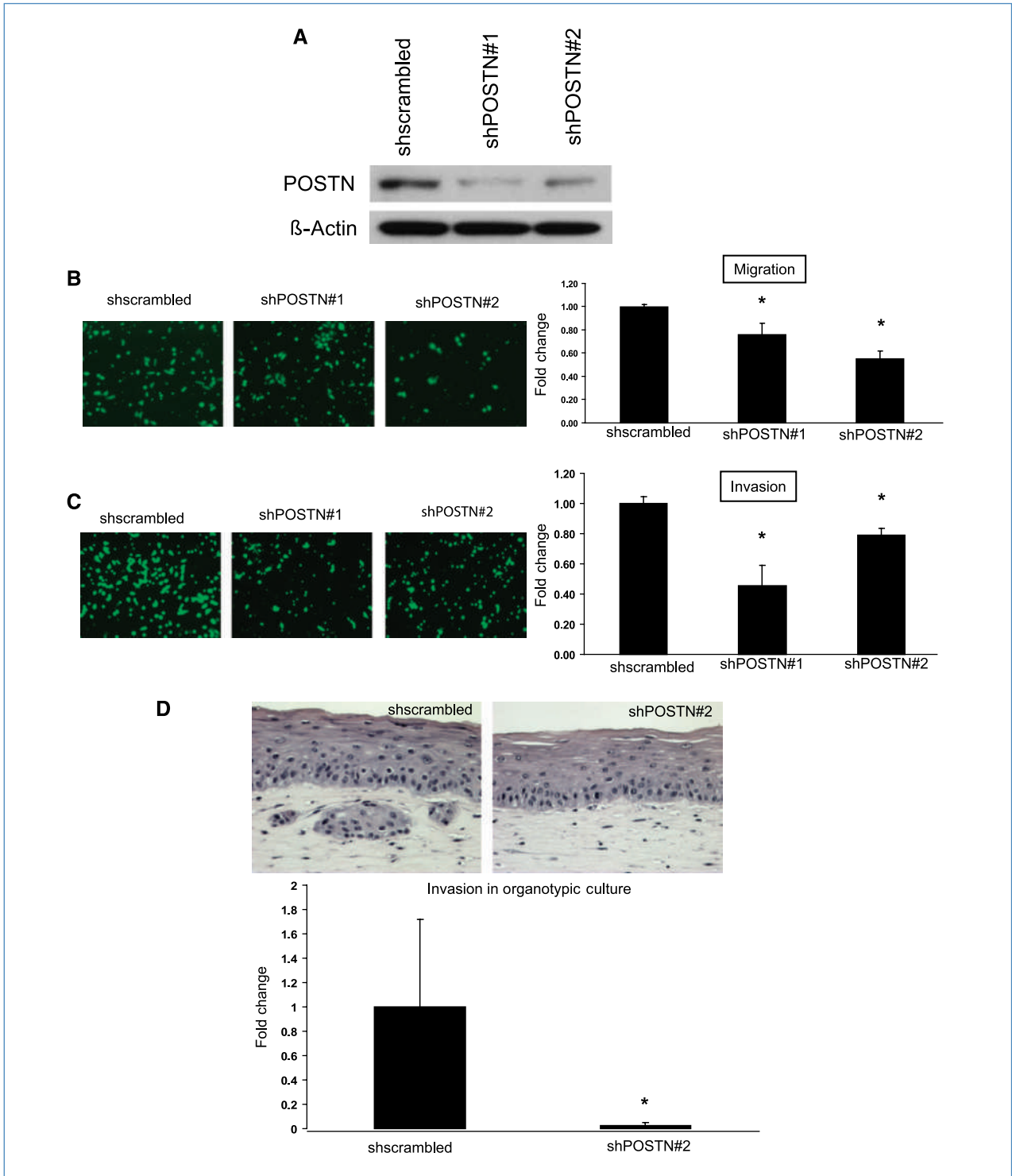


Figure 3. Periostin knockdown in EPC2-hTERT-EGFR-p53^{R175H} cells reduces migration and invasion. **A**, Western blot confirming periostin (90-kDa) knockdown in EPC2-hTERT-EGFR-p53^{R175H} cells using two independent shRNA constructs. **B**, representative fluorescent images obtained from the bottom filter of a Boyden chamber migration assay show reduced migration in EPC2-hTERT-EGFR-p53^{R175H} cells expressing shRNA to periostin versus control (scrambled) shRNA to periostin. Experiments were performed in triplicate. *, $P < 0.04$ for shPOSTN#1 versus shscrambled; *, $P < 0.001$ for shPOSTN#2 versus shscrambled. **C**, images and quantifications of the Matrigel invasion assay were acquired and processed as in **B**. Experiments were performed in triplicate. *, $P < 0.02$ for shPOSTN#1 versus shscrambled; *, $P < 0.05$ for shPOSTN#2. **D**, H&E staining of organotypic culture comparing shRNA with periostin versus scrambled shRNA showing decreased invasion of EPC2-hTERT-EGFR-p53^{R175H} cells expressing shRNA to periostin. Columns, mean fold change in invasion; bars, SEM; $P = 0.015$ ($\times 200$ magnification).

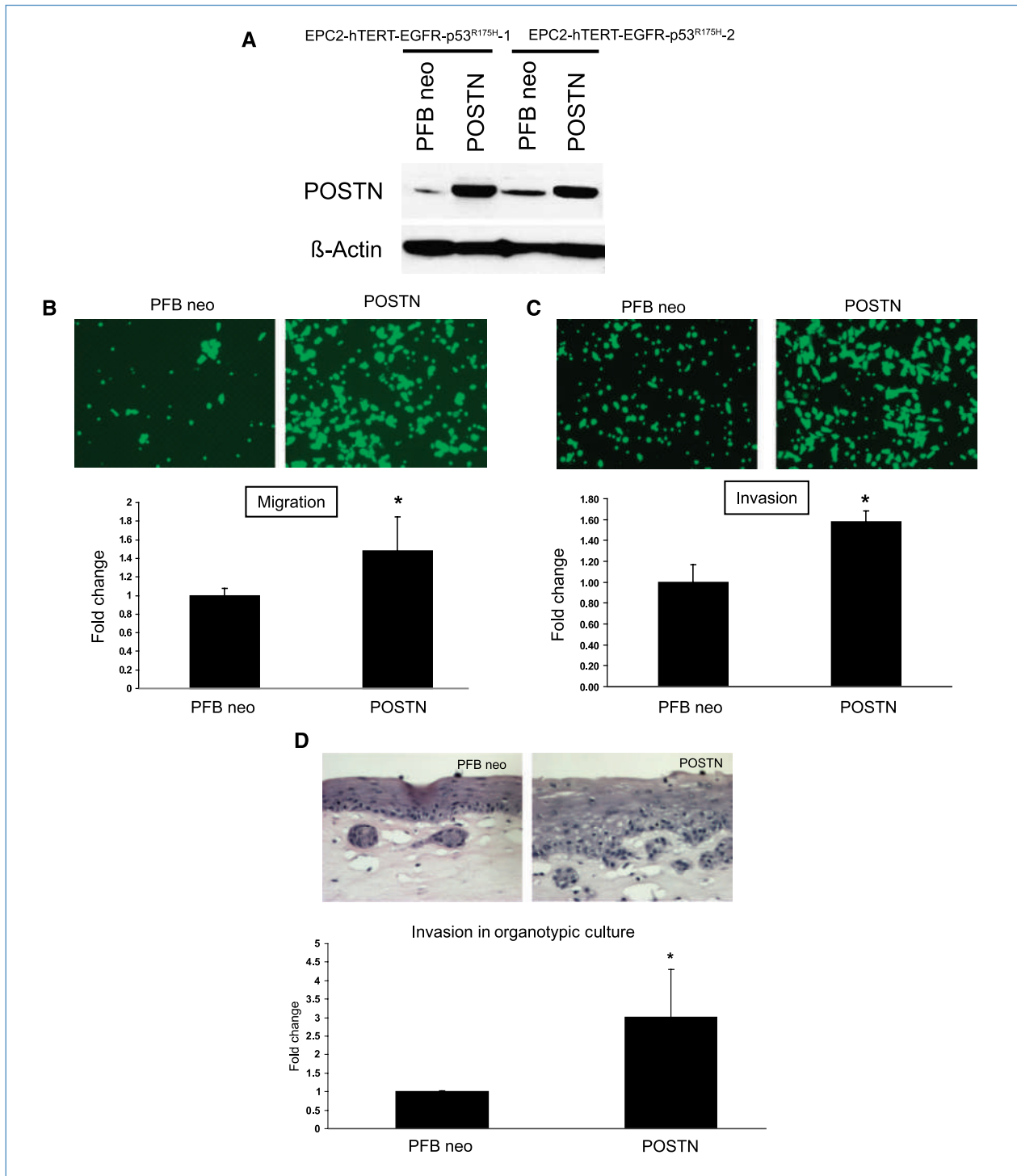


Figure 4. Periostin overexpression in EPC2-hTERT-EGFR-p53^{R175H} cells promotes increased migration and invasion *in vitro* and in organotypic culture. A, Western blot confirming periostin (90 kDa) overexpression in two independent EPC2-hTERT-EGFR-p53^{R175H} cell lines. pFB neo was used as an empty control vector. B, representative fluorescent images obtained from the bottom filter of a Boyden chamber migration assay show enhanced migration in EPC2-hTERT-EGFR-p53^{R175H} cells that overexpress periostin versus control EPC2-hTERT-EGFR-p53^{R175H}-neo cells. Columns, mean fold changes; bars, SEM; *, $P < 0.01$ (Student *t* test, EPC2-hTERT-EGFR-p53^{R175H}-periostin overexpressing cells versus control cells). Note that $P < 0.05$ is statistically significant. Experiments were done in triplicate. C, images and quantifications of the Matrigel invasion assay were acquired and processed as in B. *, $P < 0.04$. D, H&E staining of organotypic cultures comparing EPC2-hTERT-EGFR-p53^{R175H} periostin-overexpressing cells with empty vector control cells reveals increased invasion of EPC2-hTERT-EGFR-p53^{R175H} periostin-overexpressing cells. Columns, mean fold change in invasion; bars, SEM; *, $P < 0.03$ (EPC2-hTERT-EGFR-p53^{R175H} periostin-overexpressing cells versus empty control vector cells). Magnification, $\times 200$.

signaling and p53 mutation, both canonical genetic alterations in ESCC, seem to converge upon periostin based on luciferase reporter gene assays as well as inhibition of EGFR signaling and restoration of wild-type p53 function. In aggregate, these novel results underscore the utility of the organotypic culture model for the discovery of direct biological effectors of tumor invasion into the microenvironment,

which has been largely elusive to date. Local tumor invasion in the mesenchymal stromal compartment is important given that it temporally precedes tumor dissemination in the lymphatic and blood vessels for tumor metastasis.

Various avenues of investigation have highlighted the important role of the microenvironment in enhancing the initial dissemination of malignant tumor cells. Dynamic interactions

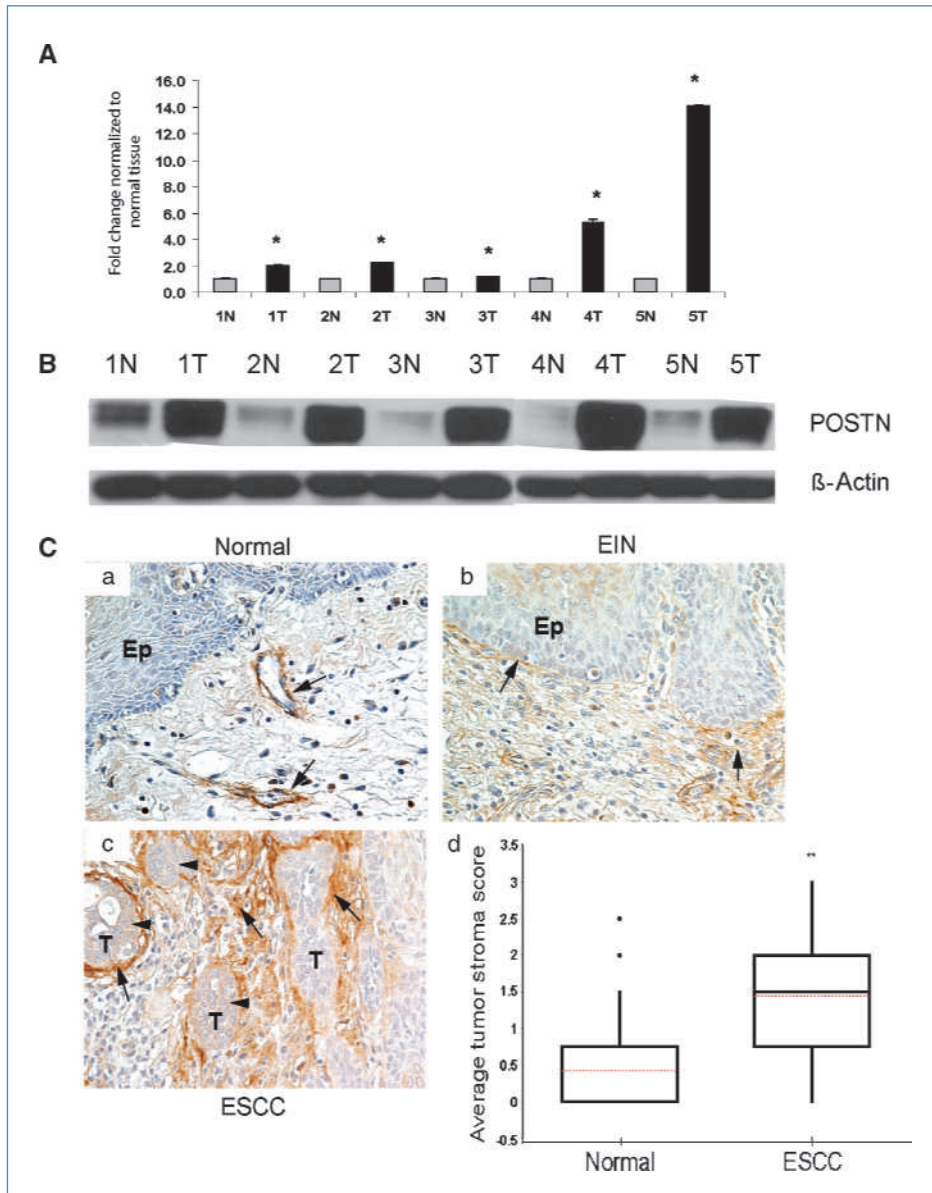


Figure 5. Periostin is overexpressed in primary ESCC tumors and is associated with ESCC tumor progression. A, relative periostin mRNA expression measured by real-time PCR in five primary ESCC tumor specimens with paired adjacent noninvasive esophageal tissue. *, $P < 0.05$. B, Western blot analysis of periostin expression in five primary ESCC tumor specimens with paired adjacent noninvasive esophageal tissue. Expression of β -actin was used as an internal loading control. C, immunohistologic analysis of a tissue microarray comprising of 73 human ESCC cases with normal esophageal tissue. Representative photomicrographs of periostin expression in normal esophageal tissue, high-grade esophageal intraepithelial neoplasia (EIN), and ESCC. Periostin expression was observed around blood vessels (left, a, arrows). Periostin staining observed in esophageal intraepithelial neoplasia epithelial-stroma interface (right, b, arrows), and accumulation in tumor stroma (bottom, c, arrows) and tumor cells (bottom, c, arrowheads). Magnification, $\times 400$. Stroma in tissue microarray was scored for periostin staining intensity, and the average score of two cores from each case were taken. ESCC cases scored higher levels of periostin expression ($n = 73$, mean = 1.44, SD \pm = 0.97) compared with matched normal controls ($n = 69$, mean = 0.44, SD \pm = 0.68; d). ●, outliers. Student's t test, ESCC cases versus matched normal esophagus controls. **, $P < 0.01$.

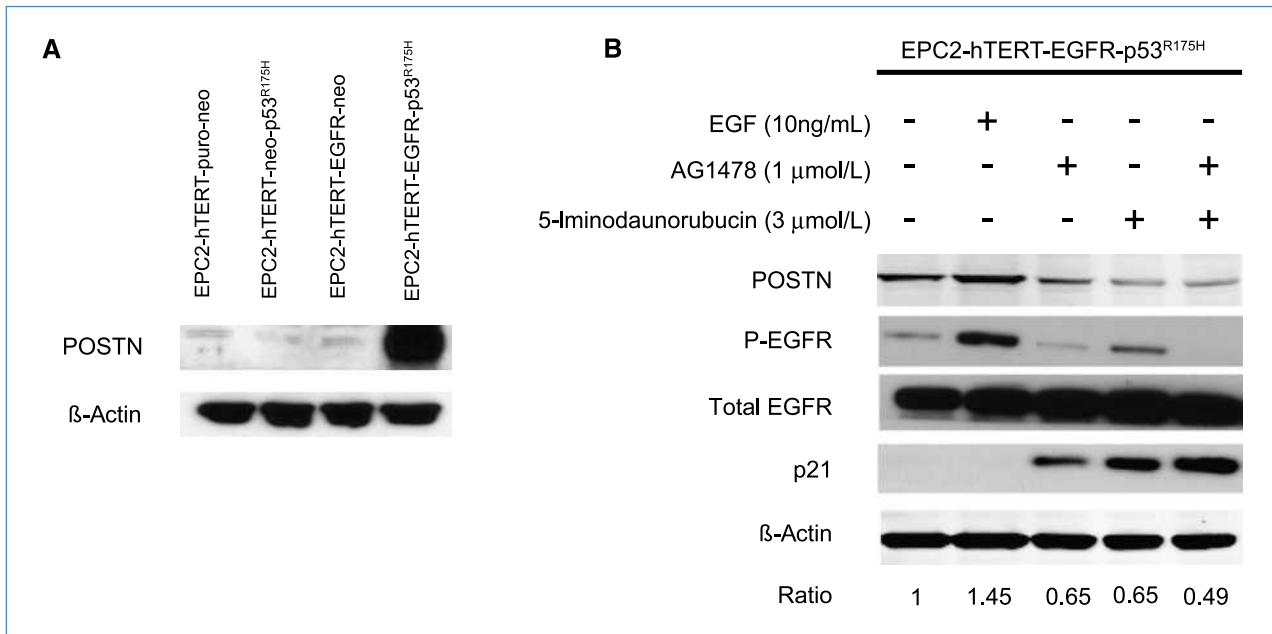


Figure 6. Periostin expression is dependent on EGFR signaling and mutant p53 activation. Western blot analysis of periostin (90 kDa) in EPC2-hTERT-EGFR-p53^{R175H}, EPC2-hTERT-puro-neo, EPC2-hTERT-EGFR-neo, and EPC2-hTERT-neo-p53^{R175H} cells. Western blot analysis of periostin expression in EPC2-hTERT-EGFR-p53^{R175H} cell lysates after 24 h of treatment with EGF (10 ng/ μ L), EGFR inhibitor AG1478 (1 μ mol/L), and 5-iminodaunorubicin (3 μ mol/L). Immunoblotting for total EGFR and phosphorylated EGFR to confirm inhibition of EGFR as well as p21 to indicate restoration of wild-type p53 signaling. β -Actin was used as a loading control. Densitometry ratios of periostin/ β -actin were calculated and recorded.

between the epithelium and mesenchymal stroma contribute to boosting the invasive phenotype of tumor cells by activating a variety of genes facilitating cell proliferation, dedifferentiation, migration, and invasion (23, 24). Significant changes such as loss of cell-cell contacts, disruptions in cell adhesion junctions, and altered cell ECM interactions within the tumor microenvironment converge to increase the ultimate metastatic potential of tumor cells (25). Therefore, identification of gene expression pattern changes during initial stages of tumor progression within the tumor microenvironment is crucial to understanding the causes of tumor invasion and, ultimately, tumor metastasis to distant organ sites. Thus, our results provide new platforms into the investigation of tumor invasion.

Periostin has been shown also to have a role in bone, tooth, and heart formation during development (26, 27) and is only reexpressed and upregulated in adult tissue after vascular, skeletal, or bone injuries (28, 29). Periostin is similarly overexpressed in human cancers (14, 30). Our results highlight that a tumor-invasive signature defines genetically engineered ESCC that is reproduced in human ESCC. Our studies also suggest that induction of periostin, a secreted protein with a long half-life (data not shown; Supplementary Fig. S4), may alter the tumor microenvironment by accumulating in the stroma and facilitating invasion through matrix remodeling. This may be achieved through the regulation of collagen I fibrillogenesis (31), serving as a bridge between tenascin C and the ECM, as well as through interaction with $\alpha_v\beta_3$ integrins. Furthermore, periostin may promote tumor cell survival in the matrix of the microenvironment by activating the Akt/

PI3K pathway. Lack of periostin may lead to the suppression of Notch1 signaling (32); conversely, it is conceivable that overexpression of periostin could activate Notch1 signaling in cancers. Indeed, we have evidence of activated Notch signaling in invasive tumor cells grown in organotypic culture (data not shown). Future translational and clinical investigations might seek to exploit periostin as an attractive therapeutic target, especially in a combinatorial fashion, for example, with inhibitors of receptor tyrosine kinases.

Disclosure of Potential Conflicts of Interest

No potential conflicts of interest were disclosed.

Acknowledgments

We thank the Morphology Core (S. Mitchell, D. Budo, and G. Swain), the Molecular Biology/Gene Expression Core (G. Wu and S. Keilbaugh), and the other members of the Rustgi laboratory for the helpful discussions.

Grant Support

NIH/National Cancer Institute P01-CA098101 (C.Z. Michaylira, G.S. Wong, A.J. Klein-Szanto, J.A. Diehl, M. Herlyn, H. Nakagawa, R. Hammond, P. Gimotty, and A.K. Rustgi), NIH/NRSA F32DK-075230 (C.Z. Michaylira), NIH T32-CA115299 (G.S. Wong), and NIH/National Institutes of Diabetes, Digestive and Kidney Diseases Center for Molecular Studies in Digestive and Liver Diseases (P30-DK050306).

The costs of publication of this article were defrayed in part by the payment of page charges. This article must therefore be hereby marked *advertisement* in accordance with 18 U.S.C. Section 1734 solely to indicate this fact.

Received 02/26/2010; revised 04/15/2010; accepted 04/22/2010; published OnlineFirst 06/01/2010.

References

- Parkin DM, Bray F, Ferlay J, Pisani P. Global cancer statistics, 2002. *CA Cancer J Clin* 2005;55:74–108.
- Nair KS, Naidoo R, Chetty R. Expression of cell adhesion molecules in oesophageal carcinoma and its prognostic value. *J Clin Pathol* 2005;58:343–51.
- Lehrbach DM, Nita ME, Cecconello I. Molecular aspects of esophageal squamous cell carcinoma carcinogenesis. *Arq Gastroenterol* 2003;40:256–61.
- Xu XC. Risk factors and gene expression in esophageal cancer. *Methods Mol Biol* 2009;471:335–60.
- Okawa T, Michaylira CZ, Kalabis J, et al. The functional interplay between EGFR overexpression, hTERT activation, and p53 mutation in esophageal epithelial cells with activation of stromal fibroblasts induces tumor development, invasion, and differentiation. *Genes Dev* 2007;21:2788–803.
- Takeshita S, Kikuno R, Tezuka K, Amann E. Osteoblast-specific factor 2: cloning of a putative bone adhesion protein with homology with the insect protein fasciclin I. *Biochem J* 1993;294:271–8.
- Horiuchi K, Amizuka N, Takeshita S, et al. Identification and characterization of a novel protein, periostin, with restricted expression to periosteum and periodontal ligament and increased expression by transforming growth factor β . *J Bone Miner Res* 1999;14:1239–49.
- Skonier J, Neubauer M, Madisen L, Bennett K, Plowman GD, Purchio AF. cDNA cloning and sequence analysis of β ig-h3, a novel gene induced in a human adenocarcinoma cell line after treatment with transforming growth factor- β . *DNA Cell Biol* 1992;11:511–22.
- Andl CD, Mizushima T, Nakagawa H, et al. Epidermal growth factor receptor mediates increased cell proliferation, migration, and aggregation in esophageal keratinocytes *in vitro* and *in vivo*. *J Biol Chem* 2003;278:1824–30.
- Harada H, Nakagawa H, Oyama K, et al. Telomerase induces immortalization of human esophageal keratinocytes without p16INK4a inactivation. *Mol Cancer Res* 2003;1:729–38.
- Calza S, Valentini D, Pawitan Y. Normalization of oligonucleotide arrays based on the least-variant set of genes. *BMC Bioinformatics* 2008;9:140.
- Benjamini Y, Hochberg Y. Controlling the false discovery rate: a practical and powerful approach to multiple testing. *JRRSB* 1995;57:289–300.
- Kudo Y, Ogawa I, Kitajima S, et al. Periostin promotes invasion and anchorage-independent growth in the metastatic process of head and neck cancer. *Cancer Res* 2006;66:6928–35.
- Siriwardena BS, Kudo Y, Ogawa I, et al. Periostin is frequently overexpressed and enhances invasion and angiogenesis in oral cancer. *Br J Cancer* 2006;95:1396–403.
- Puglisi F, Puppini C, Pegolo E, et al. Expression of periostin in human breast cancer. *J Clin Pathol* 2008;61:494–8.
- Gillan L, Matei D, Fishman DA, Gerbin CS, Karlan BY, Chang DD. Periostin secreted by epithelial ovarian carcinoma is a ligand for α (V) β (3) and α (V) β (5) integrins and promotes cell motility. *Cancer Res* 2002;62:5358–64.
- Sasaki H, Yu CY, Dai M, et al. Elevated serum periostin levels in patients with bone metastases from breast but not lung cancer. *Breast Cancer Res Treat* 2003;77:245–52.
- Sasaki H, Dai M, Auclair D, et al. Serum level of the periostin, a homologue of an insect cell adhesion molecule, as a prognostic marker in nonsmall cell lung carcinomas. *Cancer* 2001;92:843–8.
- Sasaki H, Dai M, Auclair D, et al. Serum level of the periostin, a homologue of an insect cell adhesion molecule, in thymoma patients. *Cancer Lett* 2001;172:37–42.
- Bao S, Ouyang G, Bai X, et al. Periostin potently promotes metastatic growth of colon cancer by augmenting cell survival via the Akt/PKB pathway. *Cancer Cell* 2004;5:329–339.
- Yan W, Shao R. Transduction of a Mesenchyme-specific gene Periostin into 293T cells induces cell invasive activity through epithelial-mesenchymal transformation. *J Biol Chem* 2006;281:19700–8.
- Wang W, Kim SH, El-Deiry WS. Small-molecule modulators of p53 family signaling and antitumor effects in p53-deficient human colon tumor xenografts. *Proc Natl Acad Sci U S A* 2006;103:11003–8.
- Mueller MM, Fusenig NE. Friends or foes—bipolar effects of the tumour stroma in cancer. *Nat Rev Cancer* 2004;4:839–49.
- Joyce JA, Pollard JW. Microenvironmental regulation of metastasis. *Nat Rev Cancer* 2009;9:239–52.
- Cavallaro U, Christofori G. Cell adhesion and signalling by cadherins and Ig-CAMs in cancer. *Nat Rev Cancer* 2004;4:118–32.
- Rios H, Koushik SV, Wang H, et al. Periostin null mice exhibit dwarfism, incisor enamel defects, and an early-onset periodontal disease-like phenotype. *Mol Cell Biol* 2005;25:11131–44.
- Butcher JT, Norris RA, Hoffman S, Mjaatvedt CH, Markwald RR. Periostin promotes atrioventricular mesenchyme matrix invasion and remodeling mediated by integrin signaling through Rho/PI 3-kinase. *Dev Biol* 2007;302:256–66.
- Nakazawa T, Nakajima A, Seki N, et al. Gene expression of periostin in the early stage of fracture healing detected by cDNA microarray analysis. *J Orthop Res* 2004;22:520–5.
- Lindner V, Wang Q, Conley BA, Friesel RE, Vary CP. Vascular injury induces expression of periostin: implications for vascular cell differentiation and migration. *Arterioscler Thromb Vasc Biol* 2005;25:77–83.
- Baril P, Gangeswaran R, Mahon PC, et al. Periostin promotes invasiveness and resistance of pancreatic cancer cells to hypoxia-induced cell death: role of the β 4 integrin and the PI3k pathway. *Oncogene* 2007;26:2082–94.
- Norris RA, Damon B, Mironov V, et al. Periostin regulates collagen fibrillogenesis and the biomechanical properties of connective tissues. *J Cell Biochem* 2007;101:695–711.
- Tkatchenko TV, Moreno-Rodriguez RA, Conway SJ, Molkentin JD, Markwald RR, Tkatchenko AV. Lack of periostin leads to suppression of Notch1 signaling and calcific aortic valve disease. *Physiol Genomics* 2009;39:160–8.